

Article

Study of the Reaction Mechanisms during the Thermal Decomposition of Arsenic Sulfide (V) at High Temperatures under Non-Isothermal Conditions

Kristhobal Castro ^{1,*}, Eduardo Balladares ¹, Oscar Jerez ², Manuel Pérez-Tello ³ and Álvaro Aracena ⁴¹ Department of Metallurgical Engineering, Faculty of Engineering, Universidad de Concepción, Concepción 4030555, Chile² Instituto de Geología Económica Aplicada, Universidad de Concepción, Concepción 4030555, Chile³ Department of Chemical Engineering and Metallurgy, University of Sonora, Hermosillo 83000, Mexico⁴ Escuela de Ingeniería Química, Pontificia Universidad Católica de Valparaíso, Avenida Brasil 2162, Valparaíso 2362854, Chile

* Correspondence: kriscastro@udec.cl

Citation: Castro, K.; Balladares, E.; Jerez, O.; Pérez-Tello, M.; Aracena, Á. Study of the Reaction Mechanisms during the Thermal Decomposition of Arsenic Sulfide (V) at High Temperatures under Non-Isothermal Conditions. *Minerals* **2022**, *12*, 1379. <https://doi.org/10.3390/min12111379>

Academic Editor: Chiharu Tokoro

Received: 21 August 2022

Accepted: 27 October 2022

Published: 29 October 2022

Publisher's Note: MDPI stays neutral with regard to jurisdictional claims in published maps and institutional affiliations.



Copyright: © 2022 by the authors. Licensee MDPI, Basel, Switzerland. This article is an open access article distributed under the terms and conditions of the Creative Commons Attribution (CC BY) license (<https://creativecommons.org/licenses/by/4.0/>).

Abstract: The reaction mechanisms during thermal decomposition in As-S systems are complex to describe due to the physicochemical characteristics of arsenic and its sulfides. Non-isothermal tests were carried out in a NETZSCH DTA/TG thermal analysis equipment, and interrupted tests were carried out in a vertical oven adapted for this purpose; both tests were carried out in an inert nitrogen atmosphere. The information obtained experimentally was analyzed and correlated to determine the phases and reaction mechanisms during the thermal decomposition of an arsenic sulfide (V) sample. As a result of this study, the mechanism of thermal decomposition of an arsenic sulfide sample was obtained and the apparent activation energy was determined by the Kissinger and Ozawa methods.

Keywords: reaction mechanisms; arsenic sulfide; thermal decomposition; Kissinger method; Ozawa method

1. Introduction

A large number of metallurgical processes are based on solid–gas type reactions, which generally involve several chemical reaction and diffusion stages [1], such as roasting (oxidation), preparation of metals from oxides in reducing atmospheres, nitrogenation, and metal coating, among others. The reactions of these phases are largely determined by the formation of a porous or non-porous solid product layer. If a porous product layer is formed, the reaction rate generally decreases with time due to the constant diffusion of the gas in a growing product phase [2]. According to Fan [3], a gas–solid reaction can be represented as follows:

$$aA_{(s)} + bB_{(g)} = cC_{(s)} + dD_{(g)} \quad (1)$$

While under an inert atmosphere (thermal decomposition), it can be represented as:

$$aA_{(s)} = cC_{(s)} + dD_{(g)} \quad (2)$$

During heating, the composition of sulfide minerals changes as a result of thermal decomposition or oxidation. The mechanisms responsible for such changes are not yet entirely understood, which makes it difficult to interpret the available data [4].

Furthermore, due to the vast amount of information in this regard, the data present in the literature on sulfide reaction mechanisms and kinetics show low reproducibility and great inconsistency [5], causing the tabulated values to vary depending on the source from which they are obtained [6,7].

The arsenic's physicochemical characteristics make it difficult to study its sulfides; this causes the tabulated thermodynamic values to vary between databases. In addition, this ambiguity is also a direct effect of the large number of operational and experimental variables that affect the value of the results obtained. Therefore, it is necessary to develop consistent studies that serve as a foundation for the understanding of the behavior, mechanisms, and kinetics of the thermal decomposition and oxidation of arsenic sulfide particles. It is intended that the results obtained will contribute to the existing database and/or be used as a basis for future research related to the treatment of arsenic sulfide ores.

In this research, differential thermal analysis (DTA-TG) was used, which consists of the mass sample behavior study as a function of temperature; in addition, complementary scanning electron microscopy (SEM-EDS) analyses will be used. The above is conducted in order to obtain the behavior, mechanisms, and reaction kinetics of arsenic sulfide (V) during its thermal decomposition.

2. Materials and Methods

The work consists of two stages: in the first one, the thermal decomposition of a solid granulated sample of As_2S_5 in an oxygen-free atmosphere is studied by means of non-isothermal tests; followed by a second stage of analysis of the phases formed by means of the development of Interrupted tests interrupted at established temperatures.

2.1. Sample

The sample studied corresponds to arsenic sulfide (V) from Sigma Aldrich (Merck), which has a purity of 99.8%, with a particle size of 100% $\sim 500\ \mu\text{m}$ (32 Tyler mesh) and a $P_{80} = 232\ \mu\text{m}$; this analysis was performed using a Fritsch Analysette 22 Microtec Plus laser particle size analysis equipment. Its composition was analyzed by SEM-EDS analysis in a Tescan® model VEGA II LSH scanning electron microscope equipped with a Bruker® 6030 EDS detector, where a mass percentage of 49.27% sulfur and 50.73% arsenic was quantified, which is very close to the stoichiometric composition of As_2S_5 , which contains 48.31% sulfur and 51.69% arsenic; the SEM-EDS spectrum is presented in Figure 1. This sample was homogeneously diluted in alumina at a rate of 25% As_2S_5 /75% Al_2O_3 . This technique is used to mitigate the effects caused by the volatilization of gases, in which there may be a dragging of fine particles or ejection of material out of the sample holder if a large amount of gas phase is produced; in addition, it reduces the intensity of violent reactions to limits measurable by the equipment; and in the case of reactions under the recessive core condition, by decreasing the size the particles lose contact with the walls of the sample holder, which influences the heat transfer conditions, which can be avoided by dilution. In total, 60 mg of mixture was used for each non-isothermal test; the Interrupted tests were developed with 200 mg of pure sample (without Al_2O_3 dilution).

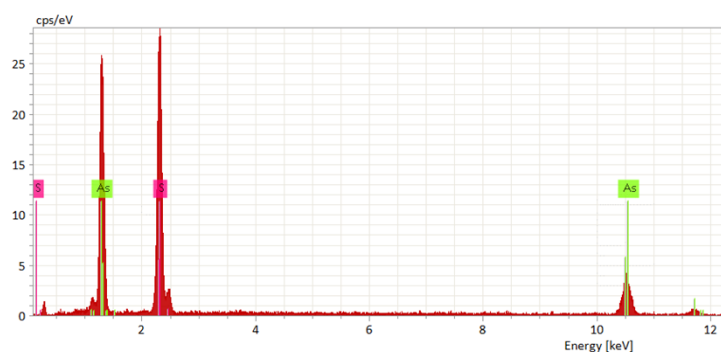


Figure 1. SEM-EDS spectrum for arsenic sulfide (V) from Sigma Aldrich (Merck) [own elaboration].

2.2. No-Isothermal

For non-isothermal thermal decomposition, the Netzsch model Jupiter STA-F449 F3 thermal analysis equipment was used, with four different heating rates (5–10–15–20 °C/min) under a dynamic atmosphere (20 mL/min) of nitrogen (99.999% N₂) in the temperature range from 25 to 700 °C. With the thermal decomposition data provided by the equipment, the methods of Kissinger [8,9] and Ozawa [10] were used to determine the apparent activation energy and kinetic parameters.

2.3. Interrupted Tests

In order to complement the non-isothermal analysis by determining the arsenical phases formed during the thermal decomposition of the sample, Interrupted tests were carried out in a vertical furnace modified for its use at temperatures 250, 300, 350, 400, 450, 500, and 600 °C. Each test consisted of injecting 1 L/min of nitrogen (99.999% N₂) from the bottom; then, suspending an alumina crucible of 11 mm internal diameter by 20 mm height with 200 mg of pure sample to the center of the furnace using a 1 mm diameter kanthal wire. Nitrogen was allowed to flow for at least 5 min to ensure the absence of oxygen inside the furnace. The furnace was then heated to the desired temperature at a standard heating rate of 30 °C/min. Once the target temperature was reached, the crucible was removed from the bottom and immediately placed in a Teflon vessel with liquid nitrogen, where the reaction was stopped for further analysis by SEM-EDS.

2.4. Gas Treatment

A tube was placed at the gas outlet to retain SO₂, by means of an aqueous solution of hydrogen peroxide, to produce sulfuric acid; while for the volatilized arsenic compounds, a spiral condenser was used in front of the absorption tube to cool the gases and transform them into solids.

3. Results and Discussion

3.1. Decomposition of As₂S₅ in Neutral Atmosphere

With the results obtained from the DTA-TG equipment, the behavior of the fraction converted, which corresponds to the mass loss of the sample as a function of temperature was analyzed and, as can be seen in Figure 2, during the thermal decomposition of the sample studied, complete conversion to the gas phase was obtained between 500 and 575 °C for the heating rates between 5 and 20 °C/min, respectively. The trend of the shift of the reactions to higher temperatures is observed as the heating rate increases, which is in agreement with Dunn [11]. In addition, three slopes are clearly seen: the first one, where the sample remains stable up to about 200 °C; subsequently, it starts to slowly increase the fraction converted up to a conversion close to 21%, which is consistent with the formation of As₂S₃ (21% mass loss). This difference is attributed to the early volatilization of elemental sulfur in the sample. Finally, on average for the four curves at a temperature of approximately 450 °C, see Figure 2; an increase in the conversion rate is observed, which is given by the rapid volatilization of a molten phase of arsenic sulfides, whose formation was visually verified when the crucible was removed at 250 °C. As can be seen in Figure 2, the reactions are displaced at higher temperatures as the heating rate increases; if the reaction is exothermic, the sample temperature will rise above that of the furnace and this effect is greater at higher heating rates. Thus, the reactions will be displaced at higher temperatures.

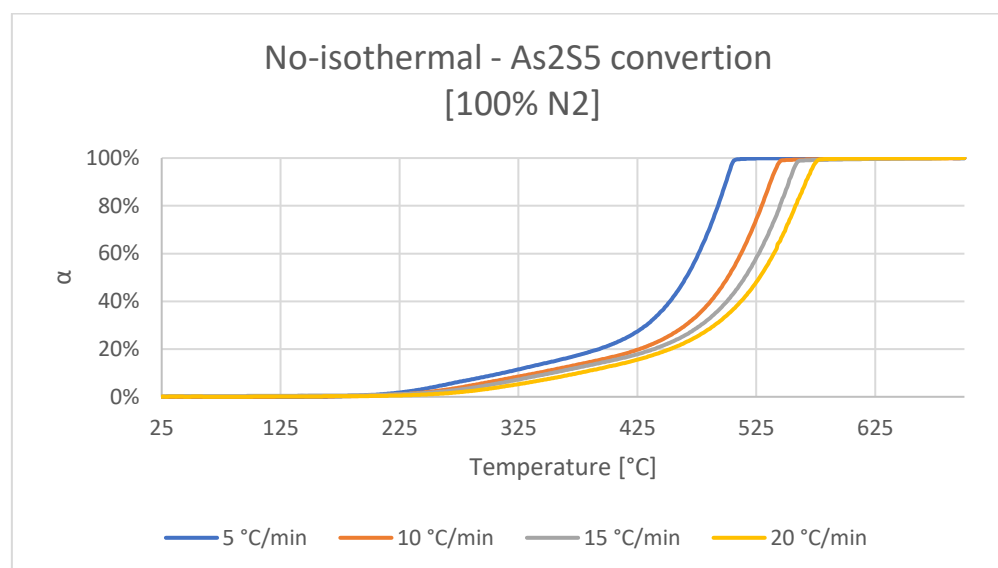


Figure 2. Fraction converted from As_2S_5 to an inert atmosphere [own elaboration].

3.2. Kinetic Parameters

To determine the activation energy, the methods by Kissinger [8,9] and Ozawa [10] are used.

3.2.1. Kissinger

The Kissinger method uses the DTG curve presented in Figure 3, obtained from the data provided by the DTA-TG equipment. The main Kissinger's formula is given by the following equation:

$$\ln\left(\frac{\phi}{T_{max}^2}\right) = -\frac{E}{R} * \frac{1}{T_{max}} + \ln\left(\frac{A * E}{R}\right) * f(\alpha_{max}) \quad (3)$$

where ϕ represents the heating rate and T_{max} the temperature at which the maximum mass loss occurs; A the frequency factor, E the activation energy, R the ideal gas constant, and $f(\alpha_{max})$ is a function depending on the converted fraction. In this method, the maximum temperature where the highest mass loss occurs is established and fixed where the peak with the highest amplitude corresponds to the highest mass loss, as shown in Figure 3. The noise present at the top of the maximum peak of some curves was attributed to the formation of a gas phase that diffuses through the alumina used to dilute the sample under study, which generates small perceptible variations due to the sensitivity of the equipment.

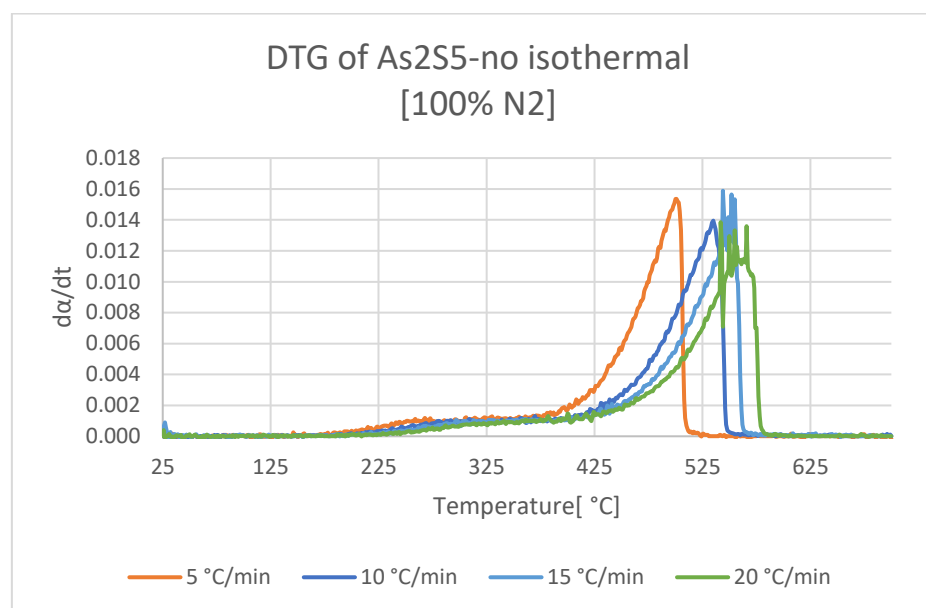


Figure 3. DTG for different heating rates in inert atmosphere. [own elaboration].

Subsequently, the temperature at which the maximum mass loss is recorded for each heating rate is plotted according to: $\ln(\phi/T_{max}^2)$ vs. $1/T_{max}$, obtaining a straight line of the form $Y = mX + C$; see Figure 4. The slope represents $-E_a/R$, where E_a represents the apparent activation energy in kJ/mol, and R is the ideal gas constant. The value of the pre-exponential factor A of the Arrhenius equation is obtained from the value of the parameter C , according to:

where $f(\alpha)$ represents the function that adjusts the values of α as a function of temperature. However, Kissinger's method [8,9] assumes that such a function is $f(\alpha)$ and its value is very close to 1, simplifying the above equation to:

$$C = \ln\left(\frac{AR}{E_a} f(\alpha_{max})\right) \quad (4)$$

The results obtained during the non-isothermal tests of arsenic sulfide (V) thermal decomposition show that the apparent activation energy has a magnitude of 108.63 kJ/mol, as can be seen in Table 1.

$$C = \ln\left(\frac{AR}{E_a}\right) \quad (5)$$

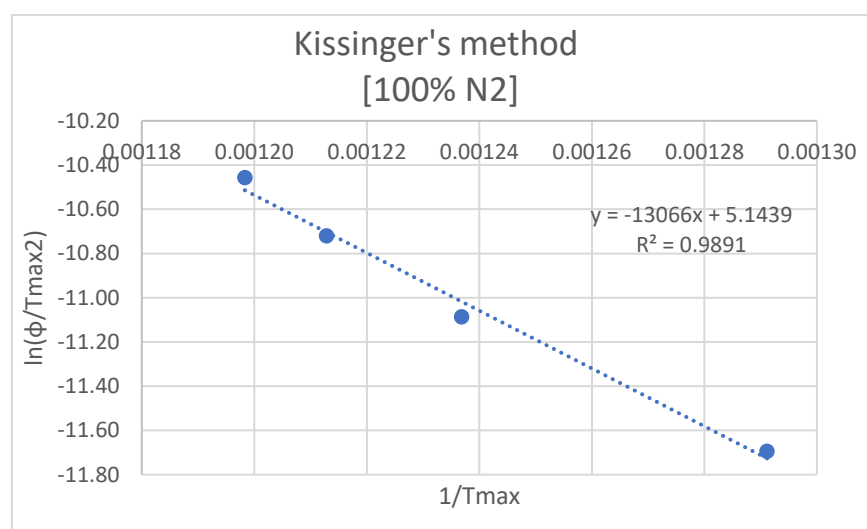


Figure 4. Kissinger’s method for thermal decomposition [own elaboration].**Table 1.** Apparent activation energy during thermal decomposition.

ϕ [K/min]	T_{max} [K]	$\ln(\phi/T_{max}^2)$	$1/T_{max}$	A [1/s]	k [1/s]
5	774.50	−11.69	1.29×10^{-3}	3.73×10^4	1.76×10^{-3}
10	808.50	−11.09	1.24×10^{-3}	3.73×10^4	3.58×10^{-3}
15	824.50	−10.72	1.21×10^{-3}	3.73×10^4	4.89×10^{-3}
20	834.50	−10.46	1.20×10^{-3}	3.73×10^4	5.92×10^{-3}
$E_a = 108.63 \text{ kJ/mol}$					

3.2.2. Ozawa

Ozawa’s method [10] uses the thermogravimetric curve, shown for each heating rate used in Figure 2, and is based on the study of the temperature at a constant mass loss for different heating rates where the converted fractions to be studied are established and kept constant for each curve or data set. The main Ozawa’s formula is given by the following equation:

$$\ln(\phi) = -\frac{E}{R} * \frac{0.4567}{T_{max}} + \ln\left(\frac{A * E}{R}\right) * g(\alpha_{max}) \quad (6)$$

where $g(\alpha_{max})$ is a function depending on the converted fraction. The converted fraction was analyzed between 10% and 100%, with a percentage step of 10%; obtaining the corresponding temperature for each converted fraction. Then, these temperatures are plotted for each heating rate according to $\ln(\phi)$ vs. $1/T$, as shown in Figure 5. The slope of each plotted curve represents the value of $-E_a/R$, multiplying each slope by $-R$, and the apparent activation energy for each percentage set is obtained. Finally, to obtain the pre-exponential factor of the Arrhenius equation, the value of the intercept C with the Y-axis of each straight line is used. For the calculation of the pre-exponential factor, it is necessary to determine a function $g(\alpha)$ that best describes the behavior of the experimentally obtained converted fraction. For the calculation of the pre-exponential factor, it is necessary to determine a function $g(\alpha)$, and be evaluated as $A = (e^C - g(\alpha)) * (R/E)$; however, it was verified that $e^C (\sim 10^6) \gg g(\alpha) (\sim 10^0)$, since this value is negligible for determining the frequency factor A from the following equation:

$$C = \ln\left(\frac{A * E}{R}\right) + \ln(g(\alpha)) \quad (7)$$

The results obtained for the apparent activation energy for the non-isothermal thermal decomposition tests of arsenic sulfide (V) can be seen in Table 2. For a mass loss of 100%, the apparent activation energy has a magnitude of 108.78 kJ/mol, very similar to that obtained by Kissinger’s method [8,9]. It should be mentioned that the values obtained by Ozawa’s method [10], as in this case, are higher; however, close to those obtained by Kissinger’s method [12].

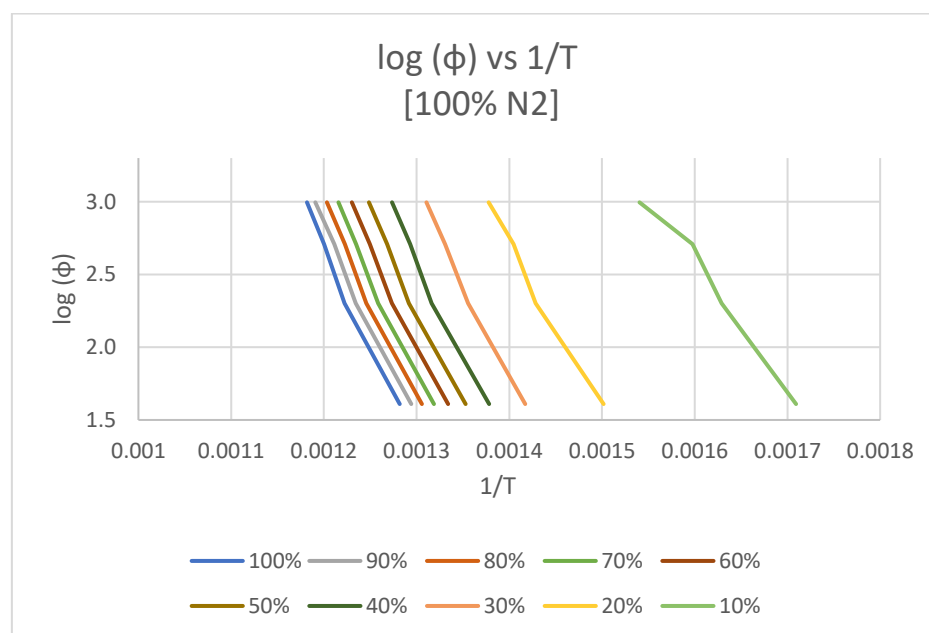


Figure 5. Ozawa's method for thermal decomposition, fixed for each percentage of mass loss [own elaboration].

Table 2. Apparent activation energy during thermal decomposition.

α [%]	10	20	30	40	50	60	70	80	90	100
Ea [kJ/mol]	66.80	88.77	102.37	103.95	104.57	105.05	105.80	106.47	105.81	108.78

3.3. Analysis of Products

These tests consisted of heating the sample to the desired temperature and quickly introducing it into liquid nitrogen to stop the reaction at the desired temperature, and to have more information on the behavior of arsenic sulfide at these temperatures, in order to determine the species present and formed during the thermal decomposition of the sample. The samples obtained were analyzed by SEM-EDS to determine the phases present and the evolution of As_2S_5 during thermal decomposition, obtaining the results shown in Table 3; and in Figure 6, which shows the micrographs obtained for each temperature studied.

For the tests developed at 600 °C, it was not possible to obtain a sample due to its rapid volatilization and the limitations in the amount of sample recovered at the end of the tests. Table 1 shows the evolution of As_2S_5 to more stable sulfides with increasing temperature, forming As_2S_3 and later, As_3S_4 .

Table 3. Summary of SEM analysis of interrupted tests in an inert atmosphere.

Temperature °C	SEM-EDS wt.-% As	SEM-EDS wt.-% S	Theoretical wt.-% As	Theoretical wt.-% S	Phase Represented
25	50.73	49.27	48.31	51.69	As_2S_5
250	60.73	39.27	60.90	39.09	As_2S_3
250	49.11	50.89	48.31	51.69	As_2S_5
300	57.66	42.34	60.90	39.09	As_2S_3
300	45.76	54.24	48.31	51.69	As_2S_5
400	59.45	40.55	60.90	39.09	As_2S_3
450	59.15	40.85	60.90	39.09	As_2S_3
500	59.37	40.63	60.90	39.09	As_2S_3

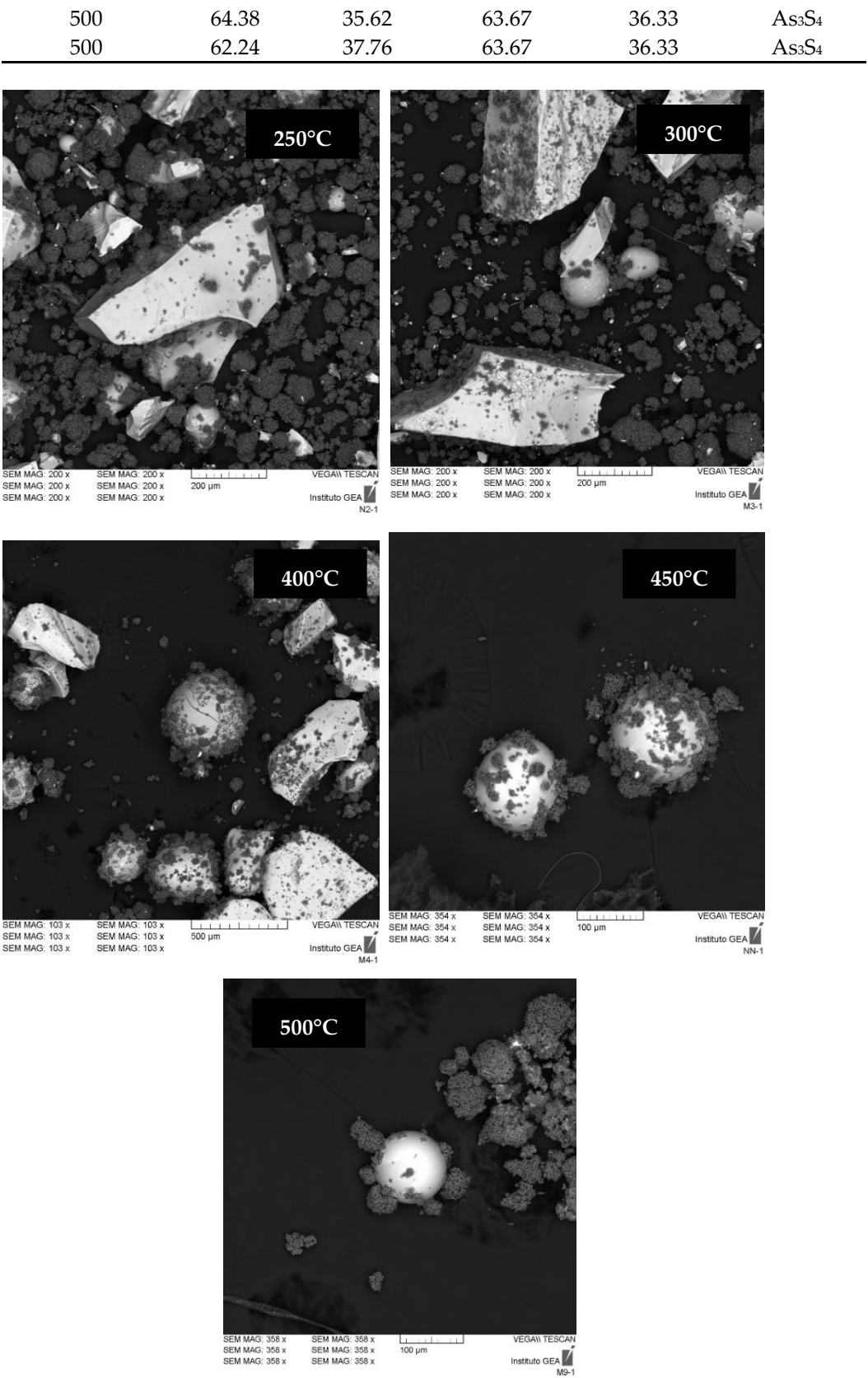


Figure 6. Micrographs obtained for each temperature studied by SEM-EDS analysis [own elaboration].

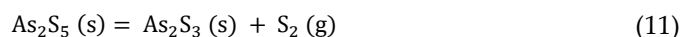
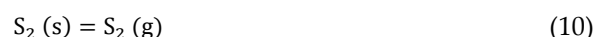
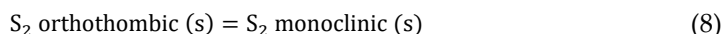
From the analyses developed and the information presented in Table 3 and Figure 6, it can be concluded that the changes that an As_2S_5 sample undergoes during its thermal decomposition are as follows:

- The As_2S_5 sample when subjected to an increase in temperature releases sulfur, transforming into As_2S_3 , a stable phase at higher temperatures;
- Subsequently, by visual inspection, it was verified that at 250 °C, there are no solids present, only a molten phase; and, given that at 300 °C, the SEM-EDS analysis detected the presence of As_2S_5 and As_2S_3 , it is inferred that the molten phase is a mixture of $\text{As}_2\text{S}_5(\text{l})$ and $\text{As}_2\text{S}_3(\text{l})$;
- After complete conversion of As_2S_5 to As_2S_3 , SEM-EDS analysis does not detect the presence of another phase between 300 and 500 °C; and
- Finally, at 500 °C, the formation of a molten As_3S_4 phase is detected, which has not been reported as part of the reaction mechanism in the literature. Therefore, the test was performed in duplicate and the same phase was detected; however, since it is consistent with the theory [11] of the formation of a stable phase at high temperatures and release of elemental sulfur, it is concluded that it is possible that As_3S_4 is a metastable transition phase, detected due to the rapid cooling in liquid nitrogen of the interrupted tests.

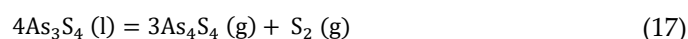
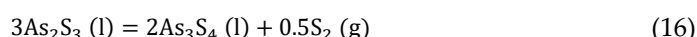
3.4. Reaction Mechanism for As_2S_5

Correlating the SEM-EDS analysis information obtained with the non-isothermal TG analyses and that presented by Castro et al. [13], the following reaction mechanism can be proposed, which is defined by temperature ranges according to the thermogravimetry tests and SEM-EDS analysis:

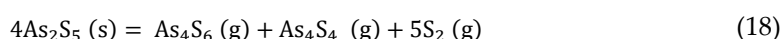
- First, decomposition between 200 and 450 °C; parallel volatilization of sulfur in the sample, along with the transformation of As_2S_5 to As_2S_3 with the sulfur release.



- Second, decomposition between 450 and 575 °C; the formation of a molten phase of metastable As_2S_3 and As_3S_4 , the latter formed from the decomposition of $\text{As}_2\text{S}_3(\text{l})$ releasing elemental sulfur. Furthermore, in this temperature range, the respective volatilizations of $\text{As}_2\text{S}_3(\text{g})$ - $\text{As}_4\text{S}_6(\text{g})$ - from $\text{As}_2\text{S}_3(\text{l})$, and $\text{As}_4\text{S}_4(\text{g})$ from $\text{As}_3\text{S}_4(\text{l})$ can be found, until a complete conversion of the sample to the gas phase.



- Finally, the overall reaction describing the thermal decomposition of As_2S_5 for a bed of 100% -500 μm particles, with a $P_{80} = 232 \mu\text{m}$, is as follows:



Subsequently, in order to verify this reaction, the HSC Chemistry software [14] was used to obtain the equilibrium constants of possible reactions for the thermal decomposition of As_2S_5 , generating Table 4, where a behavior similar to that obtained experimentally by means of the thermal decomposition tests and SEM-EDS analysis was verified. However, the HSC Chemistry software [14] neither presents information for the $\text{As}_4\text{S}_6(\text{g})$ dyad, formed from $\text{As}_2\text{S}_3(\text{g})$, nor for the As_3S_4 phase found, corroborating what was stated by Mihajlović et al. [15], who propose the lack of kinetic information regarding the behavior of arsenic sulfides. This is due to the fact that As-S systems are complex to describe since arsenic compounds have a low melting temperature [16,17]. Moreover, they sublime or decompose with the formation of more than one phase [3].

Table 4. Equilibrium constant for possible reaction mechanisms during thermal decomposition of As_2S_5 . [14].

Thermal Decomposition		
Temperature (°C)	Chemical Reaction	Equilibrium Constant K(T)
200	$2\text{As}_2\text{S}_5 = 4\text{AsS}(\text{g}) + 3\text{S}_2(\text{g})$	1.623×10^{-81}
	$2\text{As}_2\text{S}_5 = 2\text{As}_2(\text{g}) + 5\text{S}_2(\text{g})$	1.240×10^{-73}
	$2\text{As}_2\text{S}_5 = \text{As}_4(\text{g}) + 5\text{S}_2(\text{g})$	1.210×10^{-56}
	$2\text{As}_2\text{S}_5 = \text{As}_4\text{S}_4(\text{g}) + 3\text{S}_2(\text{g})$	6.768×10^{-28}
	$2\text{As}_2\text{S}_5 = \text{As}_2\text{S}_3(\text{g}) + \text{S}_2(\text{g})$	9.083×10^{-12}
300	$2\text{As}_2\text{S}_5 = 4\text{AsS}(\text{g}) + 3\text{S}_2(\text{g})$	2.972×10^{-55}
	$2\text{As}_2\text{S}_5 = 2\text{As}_2(\text{g}) + 5\text{S}_2(\text{g})$	4.553×10^{-49}
	$2\text{As}_2\text{S}_5 = \text{As}_4(\text{g}) + 5\text{S}_2(\text{g})$	2.103×10^{-36}
	$2\text{As}_2\text{S}_5 = \text{As}_4\text{S}_4(\text{g}) + 3\text{S}_2(\text{g})$	1.130×10^{-15}
	$2\text{As}_2\text{S}_5 = \text{As}_2\text{S}_3(\text{g}) + \text{S}_2(\text{g})$	2.505×10^{-6}
400	$2\text{As}_2\text{S}_5 = 4\text{AsS}(\text{g}) + 3\text{S}_2(\text{g})$	1.968×10^{-36}
	$2\text{As}_2\text{S}_5 = 2\text{As}_2(\text{g}) + 5\text{S}_2(\text{g})$	1.848×10^{-31}
	$2\text{As}_2\text{S}_5 = \text{As}_4(\text{g}) + 5\text{S}_2(\text{g})$	7.985×10^{-22}
	$2\text{As}_2\text{S}_5 = \text{As}_4\text{S}_4(\text{g}) + 3\text{S}_2(\text{g})$	1.074×10^{-6}
	$2\text{As}_2\text{S}_5 = \text{As}_2\text{S}_3(\text{g}) + \text{S}_2(\text{g})$	2.569×10^{-2}
500	$2\text{As}_2\text{S}_5 = 4\text{AsS}(\text{g}) + 3\text{S}_2(\text{g})$	3.295×10^{-22}
	$2\text{As}_2\text{S}_5 = 2\text{As}_2(\text{g}) + 5\text{S}_2(\text{g})$	3.772×10^{-18}
	$2\text{As}_2\text{S}_5 = \text{As}_4(\text{g}) + 5\text{S}_2(\text{g})$	9.431×10^{-11}
	$2\text{As}_2\text{S}_5 = \text{As}_4\text{S}_4(\text{g}) + 3\text{S}_2(\text{g})$	9.447
	$2\text{As}_2\text{S}_5 = \text{As}_2\text{S}_3(\text{g}) + \text{S}_2(\text{g})$	3.343×10^1
600	$2\text{As}_2\text{S}_5 = 4\text{AsS}(\text{g}) + 3\text{S}_2(\text{g})$	4.944×10^{-11}
	$2\text{As}_2\text{S}_5 = 2\text{As}_2(\text{g}) + 5\text{S}_2(\text{g})$	1.089×10^{-7}
	$2\text{As}_2\text{S}_5 = \text{As}_4(\text{g}) + 5\text{S}_2(\text{g})$	5.203×10^{-2}
	$2\text{As}_2\text{S}_5 = \text{As}_4\text{S}_4(\text{g}) + 3\text{S}_2(\text{g})$	3.577×10^6
	$2\text{As}_2\text{S}_5 = \text{As}_2\text{S}_3(\text{g}) + \text{S}_2(\text{g})$	1.084×10^4

4. Conclusions

The apparent activation energy was determined by Kissinger's and Ozawa's methods, obtaining 108.63 and 108.78 kJ/mol, respectively.

For the $\text{As}_2\text{S}_5(\text{s})$ sample studied, it decomposes to $\text{As}_2\text{S}_3(\text{s}, \text{l})$ until its complete conversion to the gas phase as $\text{As}_2\text{S}_3(\text{g})$ - $\text{As}_4\text{S}_6(\text{g})$ -, with the formation of a metastable phase of $\text{As}_3\text{S}_4(\text{l})$ under an inert atmosphere, obtaining the following reaction mechanism for a particle size range of 100%–500 μm , with a $P_{80} = 232 \mu\text{m}$.

This was verified with the HSC Chemistry software [14] using the equilibrium constants of possible reactions for the decomposition of As_2S_5 .

Author Contributions: Conceptualization, Á.A., O.J., E.B., and K.C.; methodology, Á.A., O.J., E.B., and K.C.; formal analysis, Á.A., O.J., E.B., K.C., and M.P.-T.; resources, Á.A., O.J., and E.B.; writing—original draft preparation, K.C.; writing—review and editing, Á.A., O.J., E.B., M.P.-T., and K.C.; supervision, Á.A., O.J., E.B., and K.C.; funding acquisition, Á.A., O.J., and E.B. All authors have read and agreed to the published version of the manuscript.

Funding: This research and the APC were funded by ANID FONDECYT INICIACION, grant number 11180432.

Data Availability Statement: Data presented in this study are available upon request from the corresponding author.

Acknowledgments: The authors thank ANID FONDECYT INICIACIÓN, 11180432 project.

Conflicts of Interest: The authors declare no conflict of interest.

References

1. Sichen, D.; Seetharaman, S. Modelling of gas-solid and solid-solid reaction kinetics. In Proceedings of the Sohn International Symposium Advanced Processing of Metals and Materials, San Diego, CA, USA, 27–31 August 2006.
2. Barnes, P. *Reactions in the Solid State*; Bamford, C.H., Tipper, C.F.H., Eds.; (Comprehensive Chemical Kinetics); Elsevier: Amsterdam, The Netherlands, 1980; Volume 22.
3. Yuanhua, F. Cinética y Mecanismos de Vaporización de Sulfuros de Arsénicos desde concentrados de cobre. Tesis Magister, Universidad de Concepción, Concepción, Chile, 1997.
4. Vershinin, A.D.; Selivanov, E.N. Thermal expansion of arsenopyrite in helium and air. *Inorg. Mater.* **2000**, *36*, 551–555. <https://doi.org/10.1007/bf02757951>.
5. Berg, L.G.; Shlyapkina, E.N. Characteristic features of sulphide mineral DTA. *J. Therm. Anal.* **1975**, *8*, 417–426. <https://doi.org/10.1007/bf01910120>.
6. Johnson, G.K.; Papatheodorou, G.N.; Johnson, C.E. The enthalpies of formation and high-temperature thermodynamic functions of As₄S₄ and As₂S₃. *J. Chem. Thermodyn.* **1980**, *12*, 545–557. [https://doi.org/10.1016/0021-9614\(80\)90184-6](https://doi.org/10.1016/0021-9614(80)90184-6).
7. Štrbac, N.; Mihajlović, I.; Minić, D.; Živković, D.; Živković, Ž. Kinetics and mechanism of arsenic sulfides oxidation December 2008. *J. Min. Metall. Sect. B Metall.* **2009**, *45*, 59–67. <https://doi.org/10.2298/JMMB0901059S>.
8. Kissinger, H.E. Variation of peak temperature with heating rate in differential thermal analysis. *J. Res. Natl. Bur. Stand.* **1956**, *57*, 217. <https://doi.org/10.6028/jres.057.026>.
9. Kissinger, H.E. Reaction Kinetics in Differential Thermal Analysis. *Anal. Chem.* **1957**, *29*, 1702–1706. <https://doi.org/10.1021/ac60131a045>.
10. Ozawa, T. A New Method of Analyzing Thermogravimetric Data. *Bull. Chem. Soc. Jpn.* **1965**, *38*, 1881–1886. <https://doi.org/10.1246/bcsj.38.1881>.
11. Dunn, J.G. The oxidation of sulphide minerals. *Thermochim. Acta* **1997**, *300*, 127–139. [https://doi.org/10.1016/s0040-6031\(96\)03132-2](https://doi.org/10.1016/s0040-6031(96)03132-2).
12. Vijayan, P.P.; Puglia, D.; Jyothishkumar, P.; Kenny, J.M.; Thomas, S. Effect of nanoclay and carboxyl-terminated (butadiene-co-acrylonitrile) (CTBN) rubber on the reaction induced phase separation and cure kinetics of epoxy/cyclic anhydride system. *J. Mater. Sci.* **2012**, *47*, 5241–5253. <https://doi.org/10.1007/s10853-012-6409-z>.
13. Castro, K.; Balladares, E.; Jerez, O.; Pérez-Tello, M.; Aracena, Á. Behavior of As/As_xS_y in neutral and oxidizing atmospheres at high temperatures—An overview. *Metals* **2022**, *12*, 457. <https://doi.org/10.3390/met12030457>.
14. HSC Chemistry®[Software], version 8.2.0, Metso:Outotec, 2022. Available online: <https://www.mogroup.com/portfolio/hsc-chemistry/> (accessed on 4 January 2022).
15. Mihajlović, N.; Štrbac, N.; Živković, Ž.; Ilić, I. Kinetics and mechanism of As₂S₂ oxidation. *J. Serb. Chem. Soc.* **2005**, *70*, 869–877.
16. Pankratz, L.B.; Mrazek, R.V.; Robert, V. *Thermodynamic Properties of Elements and Oxides*; U.S. Dept. of the Interior, Bureau of Mines: Washington, DC, USA, 1982.
17. Weisenberg, I.J.; Bakshi, P.S.; Vervaert, A.E. Arsenic Distribution and Control in Copper Smelters. *JOM* **1979**, *31*, 38–44. <https://doi.org/10.1007/bf03354510>.